

# Information dynamics in small-world Boolean networks

Joseph T. Lizier<sup>1,2,3</sup>, Siddharth Pritam<sup>1</sup>  
Mikhail Prokopenko<sup>1</sup>

<sup>1</sup>CSIRO Information and Communications Technology Centre,  
Locked Bag 17, North Ryde, NSW 1670, Australia

<sup>2</sup>Max Planck Institute for Mathematics in the Sciences,  
Inselstraße 22, 04103 Leipzig, Germany

<sup>3</sup>School of Information Technologies, The University of Sydney,  
NSW 2006, Australia

Corresponding author: Joseph Lizier  
lizier@mis.mpg.de

July 13, 2011

## Abstract

Small-world networks have been one of the most influential concepts in complex systems science, partly due to the prevalence of their occurrence in naturally occurring networks. It is often suggested that this prevalence is due to an inherent capability to store and transfer information efficiently. In this paper, we perform an ensemble investigation of the computational capabilities of small-world networks as compared to ordered and random topologies. To generate dynamic behavior for this experiment, we imbue the nodes in these networks with random Boolean functions. We find that the ordered phase of the dynamics (low activity in dynamics) and topologies with low randomness are dominated by information storage, while the chaotic phase (high activity in dynamics) and topologies with high randomness are dominated by information transfer. Information storage and information transfer are somewhat balanced (crossed over) near the small-world regime, providing quantitative evidence that small-world networks do indeed have a propensity to “combine” comparably large information storage and transfer capacity.

**Keywords:** Random Boolean Networks, phase transitions, small-world networks, distributed computation, information storage, information transfer.

## 1 Introduction

*Small-world networks* [51] have been one of the most influential concepts in complex systems science, partly due to the power of this simple concept to explain the

“six degrees of separation” phenomenon, i.e. the observation of short average path lengths in apparently highly clustered networks. Their influence has been underlined by the prevalence of their occurrence in naturally-occurring and man-made networks, e.g. in power grid networks and neural networks [51].

The structure and generation of small-world networks are well-understood; yet questions remain over what the dynamic computational properties are that make them so useful in nature. Indeed, this issue pertains to the wider field of network science: topological structure has attracted much attention [1], yet time-series dynamics are “much less well understood” [34]. Understanding the dynamics on networks is of vital importance: certainly topology gives rise to time-series dynamics on networks, but dynamics represent the specific action of a network, and only they can answer why a network is actually useful.

While much work regarding time-series dynamics has focused on state-space trajectories and damage spreading, Mitchell [34] suggests that “the main challenge is understanding the dynamics of the propagation of information ... in networks, and how these networks process such information.” This comment is typical of the speculation that remains regarding *computational properties* of networks.

In particular, much of this speculation focuses on the computational properties of small-world networks. Watts and Strogatz [51] themselves state that small-world topologies impart “enhanced signal-propagation speed” and “computational power”. Similarly, Latora and Marchiori [22] suggest that small-world networks

are prevalent in nature because they balance local efficiency and global efficiency of information transport, supported by local structure and long links respectively. Tassier and Menczer [46] infer that small-world networks emerge in a model of evolutionary labor markets as a means to transfer information, while Katare and West [18] claim that small-world structures have “maximum capability to store, process, and transfer information”.

These claims about computational properties may help to explain why small-world topologies perform better than regular lattice structures at density classification and synchronization tasks [4, 47, 48]. Yet while these claims are all based on quantitative results, they are not based on direct measurement of the relevant dynamic information quantities, either relying on measurements of topological features [18, 22] or on equating perturbation or damage-spreading type results to information transfer [46, 51].<sup>1</sup> The interest in the distributed computational properties of small-world networks, and the opportunity to properly quantify them, is the major motivating factor for our work. Indeed, appropriate measurement of these computational properties, or *information dynamics*, is possible, using a recently published framework for quantifying information storage, transfer and modification in distributed computation in complex systems [25, 27, 28, 29, 30].

In order to study the dynamics of small-world network topologies, we generate time-series activity by assigning random Boolean functions to the nodes of the networks. This approach equates to combining random Boolean networks (RBNs) with small-world topologies. We select RBNs for this purpose because of their generality as discrete dynamical network models with a very large sample space available, making them very suitable for an ensemble study of the dynamic properties provided by small-world topologies. Furthermore, RBNs are a well-studied model in the field of artificial life, due to their use as models of Gene Regulatory Networks (GRNs) [19], and the well-known phase transition they display from ordered to chaotic dynamics (in terms of length of transients in phase space with respect to average connectivity or activity level). In addition, there have been several recent studies combining RBNs with small-world topologies [31, 55]. Finally, several studies have explored the computational properties of RBNs (e.g. [37, 38]), with the behavior of information storage and transfer in RBNs being directly quantified in previous work by some of the authors [26]. In that study,

---

<sup>1</sup> While the notion may be qualitatively appealing, damage-spreading has been shown not to directly equate to information transfer, both on a theoretical basis [24] and in the applied domain of cascading failures in power grids [23], and indeed the two concepts do not have a proportional relationship.

we demonstrated maximizations of information storage and (coherent) transfer capabilities near to the order-chaos phase transition, with the two capabilities being balanced near the critical point. Given these results, and previous work indicating order-chaos transitions in dynamics as networks move from ordered to random topologies [54, 55], it seems reasonable to expect that we may observe similar maximizations of computational capabilities near a small-world transition.

In this paper, we examine the information dynamics of small-world Boolean networks from the perspective of the distributed computation undertaken by the nodes of the network in computing their attractor. We apply a recently published framework to characterize the information dynamics of the distributed computation in terms of the fundamental operations of information storage and transfer [25, 27, 29, 30]. Our perspective of computation is an important one, supported by the aforementioned related investigations in small-world networks [18, 22, 46, 51] and RBNs [37, 38], and also by wider interest in the propagation and the processing of information in networks, in particular suggesting phase transitions of these properties between ordered and chaotic regimes [20, 42]. Furthermore, this perspective provides an abstract foundation which can be generically applied to all types of time-series produced by complex networks, and as such may overcome the major problem of diversity of types of dynamical processes, which has led to the lack of a widely accepted analytical framework for network dynamics [5].

We begin by describing the network models used here, small-world networks and RBNs. We then introduce the framework for the information dynamics of distributed computation that will be used for analysis here, and describe the results of previous application to RBNs. We then outline how the small-world topology will be combined with random Boolean dynamics here, and how this will be analyzed. Subsequently, we present the results of this application, firstly generalizing our previous results to confirm that for fully-random topologies, the ordered phase of dynamics is dominated by information storage, while the chaotic phase is dominated by information transfer. Importantly, we then demonstrate that the information dynamics behave similarly in an order-chaos phase transition in dynamics as network topology undergoes an order – small-world – randomness transition. That is to say, more locally-connected, ordered networks with low activity tend to have their dynamics dominated by information storage, while more randomized networks with higher activity tend to be dominated by information transfer. Small-world networks exhibit something of a balance between these capabilities, with the capability for (coherent) information transfer being maxi-

mized near the small-world state.

## 2 Small-world Networks

The small-world network model was proposed by Watts and Strogatz [51] to explore the “six degrees of separation” phenomenon in complex networks, i.e. how apparently highly-clustered networks, similar to regular lattices, can have small average path lengths, like random graphs. The model has become one of the most influential concepts in complex systems science (e.g. see explorations in [18, 22, 31, 46, 55]), due to its ability to explain this phenomenon in a simple fashion, and the prevalence of small-world type networks in naturally occurring systems.

The model specifies how to tune networks from ordered, lattice-like structures, through small-world networks, and finally to fully-random topologies. To start, construct a regular lattice network, such as a ring lattice with  $N$  nodes where each node is connected to  $\bar{K}$  nearest neighbors. Then, rewire each edge in the network with probability  $\gamma$  (moving one end of the edge to another node selected at random). This moves the network between completely ordered at one extreme ( $\gamma = 0$ ) and completely random at the other ( $\gamma = 1$ ). To quantify the effect of these random rewirings, Watts and Strogatz [51] suggest measuring the average clustering coefficient  $C(\gamma)$  across all nodes, and the average path length  $L(\gamma)$  between all node pairs. The clustering coefficient  $C_i$  for a node  $i$  is defined as the proportion of pairs of neighbors  $j$  and  $k$  of  $i$  that have an edge. The path length  $L_{ij}$  for a node pair  $i$  and  $j$  is the length of the shortest path of edges connecting  $i$  and  $j$ .<sup>2</sup> In ordered, lattice-like networks, the high proportion of local links in these spatially embedded networks means that  $C(0)$  is high, and  $L(0)$  is large. In contrast, the lack of spatial structure in random networks means that both  $C(1)$  and  $L(1)$  are small. Intermediate values of  $\gamma$  providing very interesting results however. As shown for an example network in Fig. 3, there is a significant range of values  $\gamma$  for which the networks exhibit high clustering  $C(\gamma)$  (comparable to fully ordered networks) and small average path length  $L(\gamma)$  (comparable to fully random networks). Specifically, high  $C(\gamma)$  refers to a clustering coefficient that approaches a constant value as network size increases, while small  $L(\gamma)$  refers to logarithmic scaling of path length with system size [2, 35]. Networks in this intermediate range are labeled *small-world networks*. The convergence of these properties occurs because even a small level of randomization of

the edges creates “short cuts” across the network, which drop  $L(\gamma)$  fairly quickly with respect to  $\gamma$ . Since this occurs with a relatively small level of randomization though, the clustering  $C(\gamma)$  remains relatively high.

Following introduction of the small-world model by Watts and Strogatz [51], there was some debate on the nature of the transition between regular and random topologies. Barthélemy and Amaral [6] observed initially that the appearance of small-world behavior is not a phase transition but a crossover phenomenon which depends both on the network size and on the degree of disorder (randomization)  $\gamma$ . This was contrasted with the well-known result of Erdős and Rényi [10] stating that for random graphs there is a percolation-like transition at a specific value of the average number of links per vertex. A phase transition in small-world networks would have corresponded to the appearance of the small-world regime at a finite value of randomization  $\gamma$ . On the contrary, the crossover phenomenon between regular networks (“large worlds” with  $\gamma = 0$ ) and random networks (with  $\gamma = 1$ ) would mean that *any* finite degree of disorder  $\gamma$  is able to shift the initial lattice to the “small-world” regime as soon as the initial lattice is sufficiently large. However, the analysis of Barthélemy and Amaral [6] was shown by Newman and Watts [35] to be confined only to relatively small networks, and in fact the transition is a proper phase transition. While the existence of the transition is now well accepted, the question whether this transition is a first-order transition or a second-order transition (i.e., a continuous transition as argued by Newman and Watts [35]) is not answered easily. In particular, Argollo de Menezes et al. [3] pointed out that the small-world transition is neither a “crossover phenomenon” nor a second-order phase transition, but a first-order phase transition at  $\gamma = 0$ . This study used the normalized shortest path length distance as an “order parameter” showing that it undergoes a discontinuity in the thermodynamic limit. We shall refer to this phase transition as the *topological* phase transition driven by the randomization parameter  $\gamma$ .

Small-world networks are thought to be prevalent in nature because their clustering facilitates cooperation amongst neighbors and minimizes possibly costly long links, while their low average path length allows fast signal propagation across the network. Indeed, Watts and Strogatz [51] report faster disease spreading on small-world network models, and suggest that models with small-world coupling display enhanced “signal-propagation speed” and “computational power”. As previously outlined, Katare and West [18], Latora and Marchiori [22] and Tassier and Menczer [46] make similar claims regarding small-world networks having advanced computational capabilities, however the infor-

<sup>2</sup> The two measures can be adapted to directed networks, i.e. for  $C(\gamma)$  one considers the proportion of directed edges between pairs of neighbors that exist, and for  $L(\gamma)$  one considers the length of directed paths.

mation storage and transfer capabilities of these networks have not been directly measured.

To investigate these computational capabilities however on small-world topologies, we need an additional model to supply *time-series dynamics* to the nodes in the network. For this, we look to random Boolean networks as described in the next section.

### 3 Random Boolean Networks

*Random Boolean Networks* are a class of generic discrete dynamical network models. They are particularly important in artificial life, since they were proposed as models of gene regulatory networks by Kauffman [19]. See also Gershenson [15] for another thorough introduction to RBNs.

The RBN model specifies both the *topology* and *dynamics* of the network: while it is only dynamics that we seek to add to the small-world model, we do need to consider the relationship between the two specifications of topology.

**Topology:** An RBN consists of  $N$  nodes in a directed *network* structure. The network topology (i.e. the adjacency matrix) is determined at *random*, subject to whether the in-degree for each node is constant or stochastically determined given an average in-degree  $\bar{K}$  (giving a Poissonian distribution). It is also possible to bias the network structure, e.g. toward scale-free degree distribution [1]. Later in this paper we will be biasing the structure using the small-world model (similar to [31, 55]), noting that the use of  $\gamma = 1$  corresponds to the unbiased or fully-random RBN case.

**Dynamics:** Each node in the network has a *Boolean* state value, which is updated in discrete time. For each node, the new state value is a deterministic Boolean function of the current state values of the nodes from which it has incoming links (i.e. its neighbors). Given the topology of the network, this function or lookup table by which each node computes its next state is decided at *random* for each node when the network is initialized, subject to a probability  $r$  of producing “1” outputs. Note that  $r$  is symmetric around 0.5:  $r$  close to 1 or 0 gives low activity, close to 0.5 gives high activity. In pure RBNs, the nodes here are heterogeneous agents: there is no spatial pattern to the network structure (indeed there is no inherent concept of locality), nor do the nodes have the same update functions. (Though, of course either of these possibilities can arise in an RBN by chance). In classical RBNs (CRBNs), the nodes all update their states synchronously.<sup>3</sup> Fig. 1 provides an example of how the RBN dynamics operate.

<sup>3</sup> There has been some debate about the best updating scheme to model GRNs [8], and variations on the synchronous CRBN

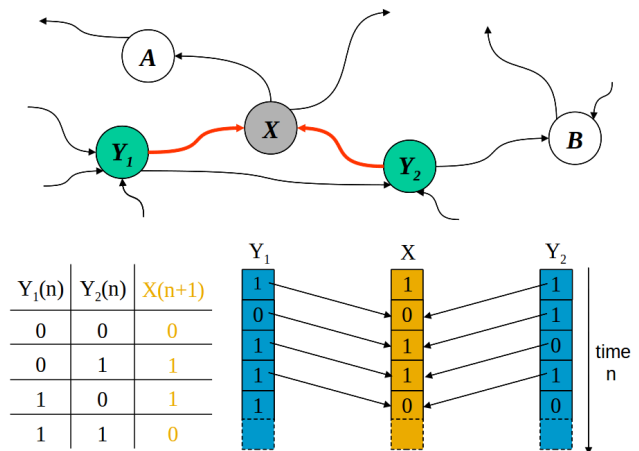


Figure 1: Example of RBN dynamics. The top part of the figure shows the position of node  $X$  in a sample RBN.  $X$  receives inputs from nodes  $Y_1$  and  $Y_2$ . The update function or lookup table for node  $X$  is shown in the bottom left, corresponding to the exclusive-OR (XOR) function:  $X = Y_1 \oplus Y_2$ . A sample time series for node  $X$ , generated via this update function from the time series of nodes  $Y_1$  and  $Y_2$ , is shown in the bottom right.

The synchronous nature of CRBNs, their Boolean states and deterministic update functions give rise to a global state space for the network as a whole, with deterministic dynamics corresponding to transient trajectories ultimately leading to either fixed or periodic attractors in finite-sized networks [52]. Effectively, the transient is the period in which the network is *computing* its steady state attractor.

RBNs are known to exhibit three distinct regimes of dynamics, depending on their parameters: ordered, chaotic and critical. At relatively low connectivity (i.e. low degree  $K$ ) or activity (i.e.  $r$  close to 0 or 1), the network is in an ordered phase, characterized by high stability of states to perturbations and strong convergence of similar macro states in state space. Alternatively, at relatively high connectivity and activity, the network is in a chaotic phase, characterized by low stability of states to perturbations and divergence of similar macro states. In the critical regime (the *edge of chaos* [21]), there is percolation in nodes remaining static or updating their values, and uncertainty in the convergence or divergence of similar macro states.

There are a number of ways to study the critical

model are known to produce different behaviors. However, the relevant phase transitions are known to exist in all updating schemes, and their properties depend more on the network size than on the updating scheme [16]. As such, the use of CRBNs is justified for ensemble studies such as ours [17].

regime, and it has been shown that there is a second-order phase transition both with respect to activity  $r$  and average connectivity  $\bar{K}$ . For example, Luque et al. [32] contrasted different order parameters: (i) the normalized Hamming distance obtained by means of Derriida’s annealed approximation [9], (ii) Flyvbjerg order parameter defined via the asymptotic stable core [13], and some others, with (iii) the percent of 1’s in the Jacobian matrix that represents the Boolean derivative of the system, and observed that all these parameters undergo a continuous change in the vicinity of critical activity  $r$ .

Similarly, it can be shown that there is a second-order phase transition near critical average connectivity  $\bar{K}$ : for example, there is a continuous phase transition in terms of the frozen component, defined as the fraction of nodes that do not change their state along an attractor, as shown by Rohlf and Bornholdt [39].

In order to distinguish the phase transitions defined in terms of a state-based parameter changing with respect to both  $r$  and  $\bar{K}$  from the topological phase transition defined in terms of a topological characteristic (such as normalized path length) changing with respect to randomization parameter  $\gamma$ , we shall refer to the state-based changes as *dynamical* transitions.

To quantify the dynamical phase transitions in the  $r$ - $\bar{K}$  phase space we shall use the well-known state-based measure of sensitivity to initial conditions, or damage spreading — that is, the normalized Hamming distance.

Following Gershenson [17], we take a random initial state  $A$  of the network, invert the value of a single node to produce state  $B$ , then run both  $A$  and  $B$  for many time steps (enough to reach an attractor is most appropriate). We then use the normalized Hamming distance:

$$D(A, B) = \frac{1}{N} \sum_{i=1}^N |a_i - b_i|, \quad (1)$$

between  $A$  and  $B$  at their initial and final states to obtain a convergence/divergence parameter  $\delta$ :

$$\delta = D(A, B)_{t \rightarrow \infty} - D(A, B)_{t=0}. \quad (2)$$

(Note  $D(A, B)_{t=0} = 1/N$ ). Finding  $\delta < 0$ , implies the convergence of similar initial states, while  $\delta > 0$  implies their divergence. In infinitely-sized networks, for fixed  $r$  the critical value of  $\bar{K}$  between the ordered and chaotic phases is [9]:

$$K_c = \frac{1}{2r(1-r)}. \quad (3)$$

For  $r = 0.5$ , we have  $K_c = 2.0$ .

To re-iterate, the phase transition in dynamics can be observed while holding activity level  $r$  constant and altering the topology via  $\bar{K}$ , or holding the topology  $\bar{K}$  constant (for  $\bar{K} > 2$ ) and altering the activity level. Also, note that order-disorder phase transitions in random Boolean dynamics have been observed for various non-random topologies, e.g. by Aldana [1] in scale-free networks while altering activity level and scale-free exponent, by Stauffer [44, 45] in regular lattices while altering activity level, and by Zhang and Zhao [55] and Lu and Teuscher [31] in small-world networks while altering network randomness, and activity and connectivity respectively.

Finite network size  $N$  is known to have an effect on the locations of the ordered and chaotic phases. For example, the sign change of  $\delta$  moves from the values of  $\bar{K}$  given by Eq. (3) slightly higher into the apparently chaotic regime for finite-sized networks [16]. More profound finite- $N$  effects include slower increases of  $\delta$  in the chaotic regime [16], and a larger shift of other indicators of the critical regime into the apparently chaotic phase (e.g. [38]). Similarly, the standard deviation  $\sigma_\delta$  of  $\delta$  is maximized slightly inside the chaotic regime for finite-sized networks [16]. When maximized, this measure indicates the widest diversity of networks for the given parameters [16], and for this reason a similar measure of *uncertainty* of avalanche size [37] has been used as an indicator of the critical regime. While other indicators of the critical regime are available that are not affected by finite-network size (e.g. the characteristic connectivity of Rohlf et al. [40]), we know that information-theoretic measures of RBN dynamics do shift with network size [38]: as such, we need to use an indicator of the critical regime that shifts with network size in order to properly guide us as to how the behavior of information-theoretic measures relates to the ordered and chaotic phases of behavior. Therefore, we select the standard deviation  $\sigma_\delta$  of  $\delta$  as guide to the relative regions of dynamics in finite- $N$  networks.

Finally, we note that much has been speculated on the possibility that gene regulatory and other biological networks function in (or evolve to) the critical regime (see Gershenson [15]). It has been suggested that computation occurs more naturally with the balance of order and chaos there [21], possibly with information storage, propagation and processing capabilities maximized [19]. In previous work, to be discussed in the next section, we sought to directly measure these computational properties, with a thorough quantitative study of the information dynamics in RBNs.

## 4 Information dynamics

Information theory [33] is the natural domain to look for a framework to describe information storage and transfer in complex systems. The fundamental quantity is the (Shannon) *entropy*, which represents the uncertainty in a sample  $x$  of a random variable  $X$ :  $H_X = -\sum_x p(x) \log_2 p(x)$  (all with units in bits). The *joint entropy* of two random variables  $X$  and  $Y$  is a generalization to quantify the uncertainty of their joint distribution:  $H_{X,Y} = -\sum_{x,y} p(x,y) \log_2 p(x,y)$ . The *conditional entropy* of  $X$  given  $Y$  is the average uncertainty that remains about  $x$  when  $y$  is known:  $H_{X|Y} = -\sum_{x,y} p(x,y) \log_2 p(x|y)$ . The *mutual information* between  $X$  and  $Y$  measures the average reduction in uncertainty about  $x$  that results from learning the value of  $y$ , or vice versa:  $I_{X;Y} = H_X - H_{X|Y}$ . The *conditional mutual information* between  $X$  and  $Y$  given  $Z$  is the mutual information between  $X$  and  $Y$  when  $Z$  is known:  $I_{X;Y|Z} = H_{X|Z} - H_{X|Y,Z}$ . Finally, the *entropy rate* is the limiting value of the entropy of the next state  $x$  of  $X$  conditioned on the previous  $k-1$  states  $x^{(k-1)}$  of  $X$ :  $H_{\mu X} = \lim_{k \rightarrow \infty} H[x|x^{(k-1)}] = \lim_{k \rightarrow \infty} H_{\mu X}(k)$ .

We have previously proposed a framework for the local information dynamics of distributed computation [25, 27, 28, 29, 30]. The framework describes computation in terms of information storage, transfer and modification at each spatiotemporal point in a complex system.

The *information storage* of an agent in the system is the amount of information in its past that is relevant to predicting its future. The *excess entropy* is the total information stored by the agent [11], while the *active information storage* is the stored information that is currently in use in computing the next state of the agent [25]. We focus on the active information since it yields an immediate contrast in the relative contributions of storage and transfer to each computation. The *active information storage* for agent  $X$  is defined as the average mutual information between its semi-infinite past  $x_n^{(k)}$  (as  $k \rightarrow \infty$ ) and its next state  $x_{n+1}$  at time step  $n+1$ :

$$A_X = \lim_{k \rightarrow \infty} \left\langle \log_2 \frac{p(x_n^{(k)}, x_{n+1})}{p(x_n^{(k)})p(x_{n+1})} \right\rangle, \quad (4)$$

with  $A_X(k)$  representing an approximation with finite history length  $k$ . From our computational perspective, an agent can store information regardless of whether it is causally connected with itself; i.e. for networks, this means whether or not the node has a self-link. This is because information storage can be facilitated in a distributed fashion via one's neighbors, in order to communicate with oneself [29, 30]. Finally, we note that

the local entropy for any agent is the sum of the local active information and the local entropy rate  $H_{\mu X}(k)$  (for any  $k$ ):

$$H_X = A_X(k) + H_{\mu X}(k). \quad (5)$$

In a deterministic system such as Boolean networks, there is no intrinsic uncertainty contained in  $H_{\mu X}(k)$ . As such, in these systems the entropy rate represents the joint contribution or transfer from the causal information sources to the destination [29, 30], though it does not specify the information transferred from any particular one of those sources.

The *information transfer* between a source and a destination agent is defined as the information provided by the source about the destination's next state that was not contained in the past of the destination. The information transfer is formulated in the *transfer entropy* (TE), introduced by Schreiber [41] to address concerns that the mutual information (as a de facto measure of information transfer) was a symmetric measure of statically shared information. The *transfer entropy* from a source agent  $Y$  to a destination agent  $X$  is the average mutual information between the previous state of the source<sup>4</sup>  $y_n$  and the next state of the destination  $x_{n+1}$ , *conditioned* on the semi-infinite past of the destination  $x_n^{(k)}$  (as  $k \rightarrow \infty$  [27]):

$$T_{Y \rightarrow X} = \lim_{k \rightarrow \infty} \left\langle \log_2 \frac{p(x_{n+1}|x_n^{(k)}, y_n)}{p(x_{n+1}|x_n^{(k)})} \right\rangle. \quad (6)$$

Again,  $T_{Y \rightarrow X}(n, k)$  represents finite- $k$  approximation. The TE can also be formulated to condition on the states  $\mathbf{v}_{x,n}^y$  of all *causal information contributors* to the destination  $X$  (the set  $\mathbf{V}_X$ ) except the source  $Y$ , so as to completely account for the contribution of  $Y$ . This formulation is known as the *complete* transfer entropy [27], defined as:

$$T_{Y \rightarrow X}^c = \lim_{k \rightarrow \infty} \left\langle \log_2 \frac{p(x_{n+1}|x_n^{(k)}, y_n, \mathbf{v}_{x,n}^y)}{p(x_{n+1}|x_n^{(k)}, \mathbf{v}_{x,n}^y)} \right\rangle, \quad (7)$$

$$\mathbf{v}_{x,n}^y = \{z_n | \forall Z \in \mathbf{V}_X, Z \neq Y\}. \quad (8)$$

The formulation in Eq. (6) is then labeled the *apparent* transfer entropy. We say that the apparent TE captures *coherent* effects from a single source only, since if a transfer effect is manifested by the interaction of two sources (e.g. an XOR-type effect), then the apparent TE cannot detect it (though the complete TE can). The entropy rate  $H_{\mu X}$  can be shown to be a sum of transfer

<sup>4</sup>The TE can be formulated using the  $l$  previous states of the source. However, where only the previous state is a causal information contributor (as for RBNs), it is sensible to set  $l = 1$  to measure direct transfer only at step  $n$ .

entropy terms, from each source to the destination one at a time and conditioning out previously considered sources; the first term is an apparent TE, the rest are higher-order TE terms conditioning on other sources (while the last is a complete TE since it conditions our all other sources) [28, 30]. Importantly, the transfer entropy properly measures a directed, dynamic flow of information, unlike mutual information measures used by Ribeiro et al. [38] and Solé and Valverde [42] which measure correlations only.

We presented the *separable information* for studying *information modification* in [28], however note that it will not be studied here.

This framework was applied to cellular automata (CAs), which are effectively an ordered lattice-style sub-class of RBNs [52], in [25, 27, 28, 29, 30]. The framework quantified blinkers and regular domains as the dominant information storage elements, particles (gliders and domain walls) as the dominant information transfer agents, and particle collisions as the dominant (non-trivial) information modification events. These results align with existing conjectures on the nature of distributed computation in CAs, providing significant impetus for the use of this framework to analyze computation in other complex systems.

Subsequently, the framework was applied to RBNs (with completely *random* topologies) [26]. It was observed that, for a fixed  $r = 0.5$ , as connectivity  $\bar{K}$  increases, the active information  $A_X$  rises within an ordered phase before reaching a maximum near to the critical point ( $\bar{K} = 2$ ) after which it falls away. At the same time, the entropy rate  $H_{\mu X}$  begins to rise only near the critical point, continuing to increase much more during the chaotic phase, approaching the level of the total entropy  $H_X$ . As captured by Eq. (5), these two components (active information and entropy rate) sum up to total entropy of the system. Therefore, the rise of  $A_X$  before the critical point indicates that the ordered phase is dominated by information storage (information contained in the past of the node about its next state). Similarly, the significant rise of the entropy rate (reaching up to the total entropy) in the chaotic phase indicates that the chaotic phase is dominated by information transfer (information from incoming links about the next state which was not contained in the nodes past). Near the critical point, there is a balance between information storage and information transfer. The apparent transfer entropy, capturing coherent transfer, is maximized within the chaotic phase near to the critical point. As the dynamics become more chaotic, the transfer component becomes more dominated by interaction rather than coherent single-source effects, and so the apparent TE reduces while the complete TE continues to increase.

We note studies of related information-theoretic measures in RBNs by Oosawa and Savageau [36] (entropy and mutual information), and in coupled RBNs by Damiani et al. [7] (mutual information and transfer entropy), though those studies focus on attractor cycles.<sup>5</sup>

## 5 Method: information dynamics analysis of small-world Boolean networks

In this study, we seek to measure the *average* information dynamics of small-world Boolean networks as a function of average in-degree or connectivity  $\bar{K}$ , activity level  $r$  and (the small-world parameter) rewiring probability  $\gamma$ .

We construct networks with  $N = 264$  as follows. Starting with  $\gamma = 0$ , we construct ring-lattice networks with average in-degree  $\bar{K}$ , firstly in an *undirected* fashion (so that degree is initially equivalent to in-degree). We consider only integer and half-integer values of  $\bar{K}$ . For even integer  $\bar{K}$ , each node simply connects to  $\bar{K}/2$  nodes on either side. For odd integer  $\bar{K}$ , each node connects to  $\lfloor \bar{K}/2 \rfloor$  nodes on either side, then each node is considered in turn, and if it doesn't yet have an extra link then an extra link is added to one of the two nearest neighbors it is not yet connected to. For half-integer  $\bar{K}$ , first the network with closest even integer  $M$  is created. If  $\bar{K} = M + 0.5$ , extra links are *added* as outlined for odd integer  $\bar{K}$ , but only for half of the nodes (in a symmetric manner to keep the ring regular). If  $\bar{K} = M - 0.5$ , then one of the two outermost links are *removed* for half the nodes (in a symmetric manner). The undirected links are then converted into two *directed* links, one in each direction. Each link in the network is then rewired with probability  $\gamma$ . Except for our first investigation with a fixed  $\gamma = 1.0$ , we experiment separately with rewiring only the destination or only the source of the links.<sup>6</sup> This allows us to check for any difference in the transition with a heterogeneous distribution of in-degrees  $K$  (by rewiring the sources) or with uniform  $K$  (by rewiring the destinations). Self-links are allowed under rewiring, though they were not included in the ordered lattice. In alignment with [31] we make no attempt to keep the network strongly connected, since this is not done for ordinary RBNs, noting that this can in-

<sup>5</sup> Damiani et al. [7] use  $k = 1$  for the transfer entropy: one would find that transfer vanishes in the attractor states with  $k \rightarrow \infty$ , since at that point node behavior is completely predictable from their own pasts.

<sup>6</sup> The method described by Zhang and Zhao [55] rewires the destinations, while that of Lu and Teuscher [31] rewires the sources.

fluence the results (as per Lu and Teuscher’s analysis [31]). We confirmed that, when rewiring the sources, we obtained input degree distributions as a function of  $\gamma$  that aligned with the theoretical results obtained by Zhang and Zhao [55] (not shown).

To generate dynamics on these networks once their topology is determined, we assign each node a Boolean function of its inputs. The nodes in the network can then be initialized at random initial states, and the time-series of their behavior generated. We use synchronous updating as described earlier, and model the networks using enhancements to Gershenson’s RBNLab software [14].

We measure the average entropy, entropy rate, and active information for each node in a given network (e.g.  $A_X(k)$ ), then average these over each node in the network (to get e.g.  $\langle A_X(k) \rangle$ ), then average these network averages over many networks (at least 250) generated for each  $(r, \bar{K}, \gamma)$  set to determine the average values as a function of  $(r, \bar{K}, \gamma)$  (denoting this, e.g., as  $A_X(r, \bar{K}, \gamma)$ ).<sup>7</sup> Similarly, the average apparent and complete transfer entropies are measured for (at least 50) randomly sampled pairs<sup>8</sup> of causally linked nodes (unlike the mutual information measurements by Ribeiro et al. [38] and Solé and Valverde [42] for any, not necessarily linked, node pairs), averaged once to obtain network averages, and again over many networks to obtain averages as a function of  $(r, \bar{K}, \gamma)$ .

We seek to approximate an infinitely-sized network, and so avoid running the network for too many time steps because the computation is completed once the network reaches a periodic or fixed attractor (inevitable for finite-sized Boolean networks). For each simulation from an initial randomized state, we ignore a short initial transient of 30 steps, then observe another 400 time steps (similar to the approach in [53]). We do not explicitly limit the observations to the attractor states, since this would artificially inflate the observed activity in ordered networks. Instead, we use the same number of observations for each network, and using 400 time steps for this network size allows the focus to remain on the transient. Ignoring the first 30 states allows the network to settle into the main phase of the computation and avoids the observation of global states that are highly unlikely to dynamically occur.

Importantly, since the nodes in each network are heterogeneous agents, the probability distribution func-

tions for each measure must be computed for each node individually rather than combining observations across all nodes (as could be done for the homogeneous agents in CAs, e.g. [27]). In order to properly sample the dynamics of each node in each RBN and generate enough data for the information-theoretic calculations, many repeat runs from random initial states are required for each network (at least 4480 are used). For these calculations, one should use as large a history length  $k$  as facilitated by the number of observations [27, 30]; here we find  $k = 13$  provides reasonable convergence (qualitatively observed) for a reasonable number of repeat runs (in the time available for experimentation).

In examining *average* computational properties as a function of network parameters, we emphasize that there is in general a very large range of network realizations and consequently of behaviors possible for each parameter set. The local information dynamics of computation will provide much more detailed insights *for a given* network (as for CAs in [27]) than averages over nodes, networks and network sets discussed here. That being said, these averages can provide important insights into the computational properties as a function of network parameters, so long as we remember that the average results are akin to likelihoods rather than certainties, albeit likelihoods that are much stronger in the limit of infinite system size.

## 6 Results and discussion

While presenting the following results we keep the distinction between (a) the *topological* phase transition from ordered to random networks defined in terms of topological characteristics changing with respect to the randomization parameter  $\gamma$ , and (b) the *dynamical* phase transitions from ordered to chaotic phases, defined in terms of state-based changes with respect to both  $r$  and  $\bar{K}$ , as well as  $\gamma$ .

### 6.1 Dynamical phase transitions in RBNs

In order to validate the model, we begin our analysis with the case of completely random networks ( $\gamma = 1.0$ ). That is, we focus our attention on the dynamical order-chaos phase transition with respect to both activity  $r$  and connectivity  $\bar{K}$  in networks without the small-world structure. Here, the randomization with  $\gamma = 1.0$  rewires only the destination of links, aligning with the use of non-uniform in-degrees in our earlier investigation of RBNs [26]. As expected, the model produces extensions of the observations of our earlier work [26] which investigated the phase transition with respect to

<sup>7</sup> We leave  $k$  out of the notation here, since  $k$  is unchanged at 13 for all measurements here, and is not the focus of our attention.

<sup>8</sup> While this method of sampling linked pairs does increase the standard deviation of our network averages, the fact that we average over a large number of sample networks means that the measures display the same trends as they would if we averaged over all linked pairs. We verified this for number of parameter settings.

$K$  for fixed  $r = 0.5$ . In summary, as shown in Fig. 2:

- There is an order-chaos phase transition in dynamics, the location of which is inferred by the maximization of the standard deviation  $\sigma_\delta$  of the convergence/divergence parameter  $\delta$  (Fig. 2a). Chaotic behavior with large  $\delta$  occurs for large  $r$  and  $\bar{K}$  (in top right corner of the diagram), while ordered behavior occurs for small  $r$  and  $\bar{K}$  (in the bottom left).<sup>9</sup> Note that the transition can be seen to occur for  $\bar{K}$  with fixed  $r$ , or alternatively for  $r$  with fixed  $\bar{K}$ , except where  $\bar{K}$  is too small for chaotic dynamics to be reached for any  $r$ . The location of the transition approximates the known trajectory in Eq. (3) [9, 15] (overlayed on the plot), though is shifted to larger  $\bar{K}$  and towards  $r = 0.5$  due to the finite network size;
- Total entropy increases into the chaotic regime (Fig. 2b);
- Information storage dominates the ordered phase (Fig. 2c), accounting for almost all of the information  $H_X$  in the next state (Fig. 2b) there. In contrast, transfer captured in total in the entropy rate (Fig. 2d) dominates the chaotic phase, accounting for almost all of the information  $H_X$  in the next state (Fig. 2b) in that regime;
- Information storage peaks just inside the ordered phase (Fig. 2c), while apparent transfer entropy (capturing coherent effects) peaks just inside the chaotic regime (Fig. 2e);
- As dynamics move more deeply into the chaotic phase, higher order interactions begin to dominate — apparent TE decreases from its peak as the capacity for coherent computation is eroded (Fig. 2e), while more of the transfer component is carried in complete TE (Fig. 2f). These findings add important evidence to the conflicting conjecture over whether information transfer is found at an intermediate [21] or maximum level [42] at criticality. We see that for RBNs, it is maximized close to criticality where one measures the apparent influence of a source in isolation, but equally it is at an intermediate level where the measurement considers the other causal information sources also. If these findings apply to such phase transitions in general, then both sources of conjecture appear to be well-founded, being resolved in these two different methods of measuring information transfer.

<sup>9</sup> Which region is chaotic and which is ordered is inferred from the sign of  $\delta$  (not shown), though as described earlier we use the maximization of  $\sigma_\delta$  (instead of  $\delta = 0$ ) to guide us to the location of the critical regime in finite-sized networks.

## 6.2 Phase transitions in small-world networks

Having validated our model for the case of completely random networks ( $\gamma = 1.0$ ), we proceed to presenting the main part of the results, where we fix the number of connections  $\bar{K} = 4$ , vary the small-world network randomization parameter  $\gamma$  and the level of activity in the network  $r$ . We focus on results obtained from randomizing the destinations of links, and mention differences to results from randomizing the sources of links where these arise. Our aim is to investigate (i) topological phase transitions driven by changes in randomization parameter  $\gamma$ , giving rise to small-world phenomenon, and (ii) dynamical phase transitions driven by changes in the activity parameter  $r$ .

### 6.2.1 Topological phase transitions in small-world networks

In the considered system, the small-world characteristics arise with  $\bar{K} = 4$  (being independent of  $r$ ) for  $\gamma$  approximately between 0.03 and 0.1. This is illustrated by Fig. 3 which traces small-world characteristic parameters: average clustering coefficient  $C(\gamma)$  and average path length  $L(\gamma)$  (averaged for all directed node pairs where a directed path exists). As mentioned earlier, the one-sided topological phase transition in terms of the path length occurs at  $\gamma = 0$  (for infinitely-sized networks), while the change in the clustering coefficient lags behind. Whether this lag indicates yet another phase transition marking the edge of the small-world regime on the other side remains an elusive research question.

### 6.2.2 Dynamical phase transitions in small-world networks

We then explore the convergence/divergence properties of the small-world Boolean networks, measuring  $\sigma_\delta$  with respect to activity  $r$  and rewiring  $\gamma$  with  $\bar{K} = 4$ , to locate any order-chaos phase transition in dynamics. In particular, we examine phase transitions in dynamics with respect to (i)  $r$  for fixed  $\gamma$ , and then (ii) with respect to  $\gamma$  for fixed  $r$ .

The phase transition with respect to (i)  $r$  for fixed  $\gamma$  can be verified using  $\sigma_\delta$  in Fig. 4a — the ordered phase exists for low  $r$ , with the chaotic phase for large  $r$ . It is worth pointing out that the results along the line  $\gamma = 1.0$  correspond to the results for completely random networks along the line for  $\bar{K} = 4$  in Fig. 2a. We also note that when  $\gamma$  is too low (below  $\sim 10^{-2}$ ), the chaotic phase does not appear to be reached for any  $r$  with this  $\bar{K}$  (i.e. there is no transition for these param-

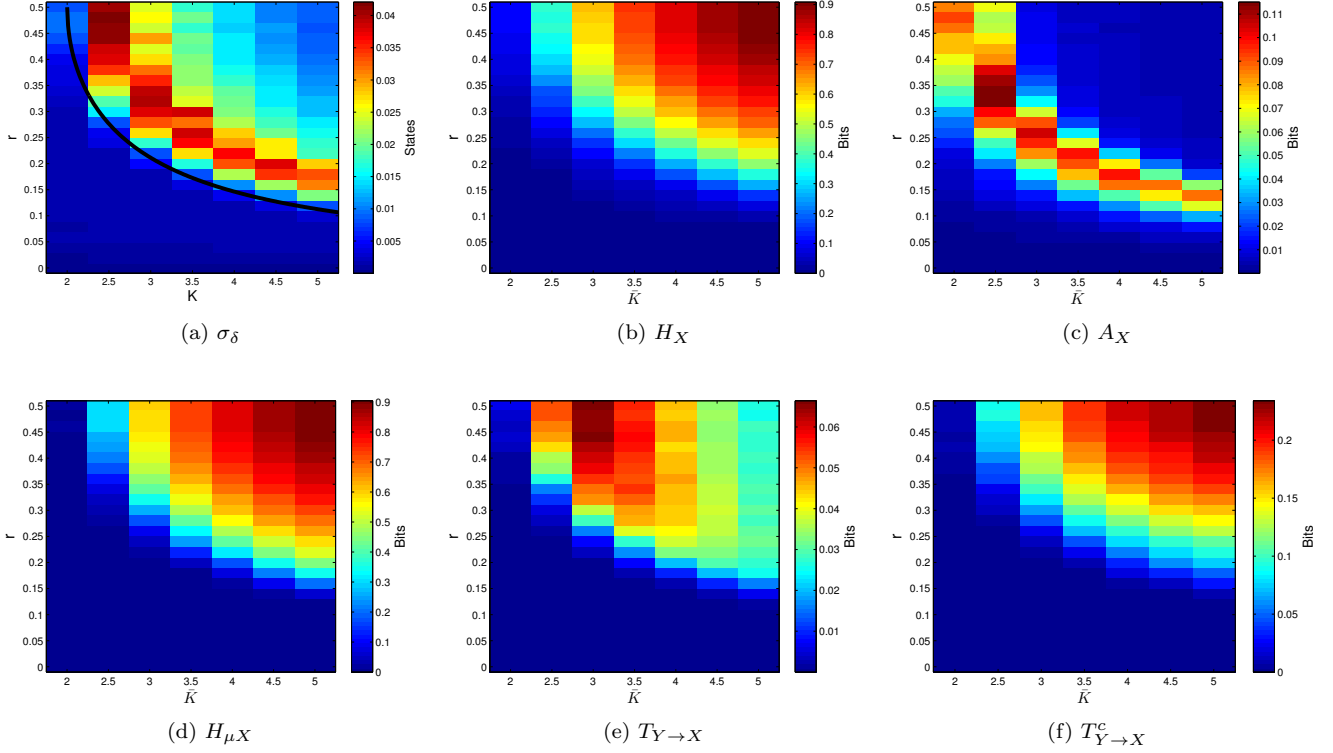


Figure 2: **Connectivity and activity driven dynamical phase transitions in RBNs** (color online). Measures of dynamics versus  $\tilde{K}$  and  $r$  for  $\gamma = 1.0$  (i.e. fully randomized networks). This is akin to the standard RBN case. We plot: (a) standard deviation of the convergence/divergence parameter  $\delta$ , the maxima of which indicates the location of the critical state, with the curve of the theoretical location of the critical state for infinitely-sized networks superimposed (the sign of  $\delta$ , not shown, indicates chaotic behavior in the top right for large  $\tilde{K}$  and  $r$ , and ordered behavior for small  $\tilde{K}$  and  $r$ ); (b) average entropy; (c) average active information storage; (d) average entropy rate; (e) apparent transfer entropy; and (f) complete transfer entropy. For an indication of the scale of error bars, see Fig. 7a.

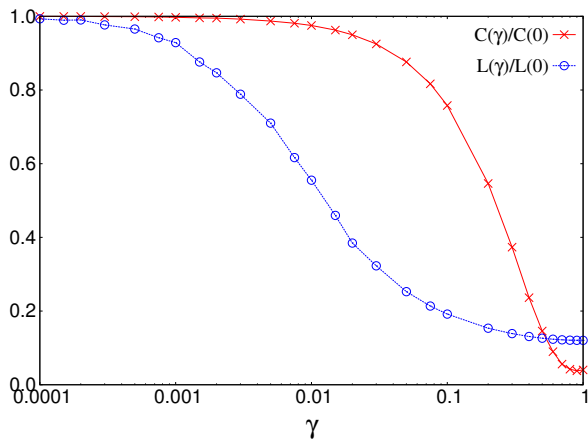


Figure 3: Small-world characteristic parameters (average clustering coefficient  $C(\gamma)$  and average path length  $L(\gamma)$ ) for the networks used here with  $K = 4$ , and the destinations of links randomized with probability  $\gamma$ . The small-world regime appears to be between  $\gamma \approx 0.03$  and 0.1.

eters).<sup>10</sup> Of course, when  $\bar{K}$  is increased, the chaotic phase can be reached for high  $r$  even for completely regular networks with  $\gamma = 0$  – see Fig. 5. This aligns with the finding of Stauffer [44, 45] that such phase transitions can occur even in completely regular networks with Boolean dynamics.

Crucially, we note that a similar transition between ordered and chaotic dynamics occurs (ii) with respect to the small-world rewiring parameter  $\gamma$  **for fixed**  $r$ .<sup>11</sup> Ordered dynamics are observed for small  $\gamma$  (roughly corresponding to ordered networks), while chaotic dynamics are observed for large  $\gamma$  (roughly corresponding to somewhat randomized networks). These results are quite intuitive: in more ordered, locally connected topologies, one can imagine that it is difficult for disturbances to spread, while the introduction of long-links could be expected to spread disturbances across the network quickly and contribute to chaotic behavior. We note though, that if  $r$  is too low (below  $\sim 0.25$  here), chaotic dynamics cannot be reached for any  $\gamma$  with this  $\bar{K}$ . While many natural GRNs may be modeled with  $\bar{K}$  and  $r$  values that would imply operation in the chaotic regime if their topology was random, the presence of small-world topology could thus mean that their dynamics are in fact closer to critical [55].

Importantly, we find that there is negligible differ-

<sup>10</sup> We note that this may be an artifact of the use of finite-sized networks.

<sup>11</sup> The exact nature of the transition with respect to  $\gamma$  in the limit of infinite network sizes is unknown, so it is unclear whether this is precisely a phase transition or crossover phenomenon.

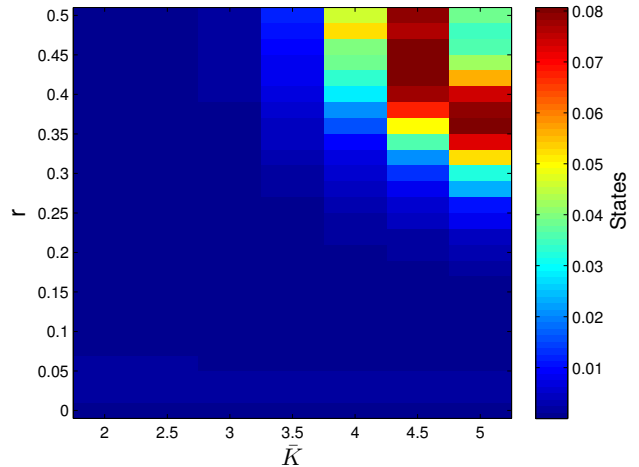


Figure 5: (color online) Standard deviation  $\sigma_\delta$  of perturbation distance  $\delta$  as a function of  $\bar{K}$  and  $r$  for fixed  $\gamma = 0.0$  (i.e. a completely regular ring network). High  $\bar{K}$  and  $r$  combinations (top right) give chaotic dynamics, small  $\bar{K}$  and  $r$  (bottom left) give ordered dynamics; the critical regime is indicated by the maximum values of  $\sigma_\delta$ .

ence in the transitions when we randomize the sources of links rather than the destinations; see Fig. 6a. While it is known that more broad in-degree distributions show more ordered behavior [55], this tendency appears to only affect the strength of behavior here rather than the location of the transition. This aligns with the work of Aldana [1], who while showing that the in-degree distribution of a network certainly has an influence on the order-disorder phase transition, suggested that scale-free networks produce the same phase diagram regardless of whether it is the input or output degree distribution that is scale-free.

There is some alignment to Lu and Teuscher [31], who found that damage spreads faster in more random networks (except for networks with very low connectivity, well-inside the ordered regime), though their study focused more on identifying the “critical connectivity of stability” (where damage spreading is independent of network size) than the “edge of chaos”.<sup>12</sup>

<sup>12</sup> Our results initially seem to differ with Zhang and Zhao [55], who found that as the rewiring probability increases “the network becomes more ordered”. This may, in part, be because that inference was based on small differences in the “active fraction” of the network rather than directly based on damage spreading, and this measure may have been influenced to a large degree by the broadening of the in-degree distribution with  $\gamma$ . Furthermore, the point in the ( $r = 0.7, \bar{K} = 3$ ) phase-space chosen by Zhang and Zhao for this inference may not properly sample the chaotic regime for any  $\gamma$  in the finite-sized ( $N = 100$ ) networks used there

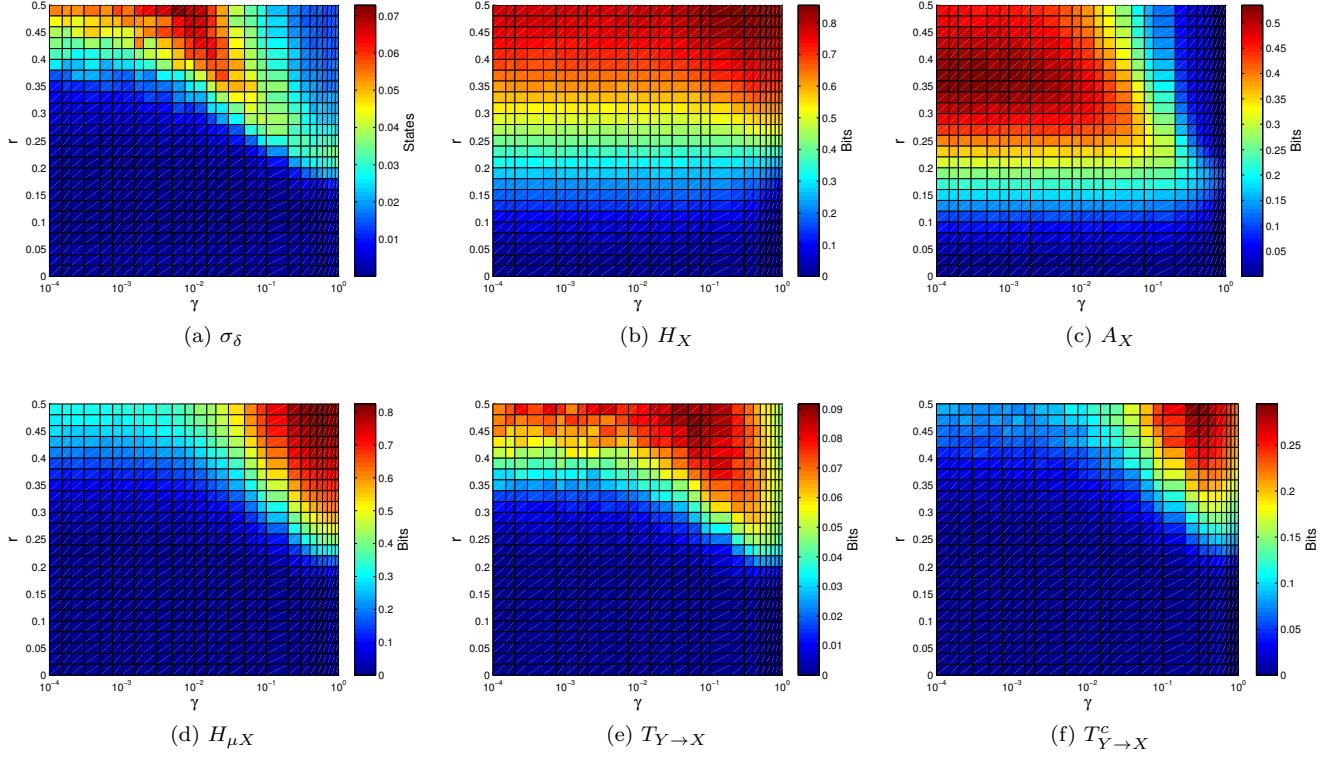


Figure 4: **Small-world and activity-driven transitions for randomized destinations** (color online). Measures of dynamics versus  $r$  and  $\gamma$  for  $K = 4$  (i.e. ordered, small-world and random networks). We plot: (a) standard deviation of the convergence/divergence parameter  $\delta$ , the maxima of which indicates the location of the critical regime (the sign of  $\delta$ , not shown, indicates chaotic behavior in the top right for large  $\gamma$  and  $r$ , and ordered behavior for small  $\gamma$  and  $r$ ); (b) average entropy; (c) average active information storage; (d) average entropy rate; (e) apparent transfer entropy; and (f) complete transfer entropy. For an indication of the scale of error bars, see Fig. 7a.

From the above, we see that all three parameters  $\bar{K}$ ,  $r$  and  $\gamma$  control the dynamics. While it is possible to see order-chaos transitions in dynamics with respect to one parameter while varying the others, we do not see the full transitions for every combination, and the location of the transition depends on all three.

Importantly, the location of the critical region in dynamics with respect to  $\gamma$  has much similarity with the location of small-world regions of  $\gamma$ . We note however, that the critical point in dynamics does not necessarily exactly line up with the range indicated by the onset of the small-world: e.g., for  $r = 0.3$  it is between  $\gamma = 0.05$  and  $0.5$ , or indeed for  $r < 0.2$  the chaotic regime does not appear to be reached for any  $\gamma$ . This highlights the importance of node behavior in forming the dynamics: they cannot be predicted from the topology alone.

### 6.2.3 Information dynamics of the dynamical phase transitions

Now we switch our analysis to information dynamics in terms of the entropy (composed as a sum of the active information storage and entropy rate), and the information transfer components (incorporating both apparent and complete TEs). This analysis will trace changes in these quantities while both  $r$  and  $\gamma$  change, as shown in Fig. 4 for destination randomization and Fig. 6 for source randomization. More detailed views of the small-world transition are presented in plots of the information dynamics versus  $\gamma$  for fixed  $r = 0.36$  and  $\bar{K} = 4$ , in Fig. 7; these views are typical of the results with respect to  $\gamma$  where  $r$  is large enough such that a transition from ordered to chaotic dynamics is observed.

We can observe some distinct behaviors of these measures through the changes, be it the small-world transition with respect to  $\gamma$ , or the phase transition driven by the dynamics  $r$ . The trends with respect to the ordered and chaotic phases of dynamics mirror those for the order-chaos transitions in standard RBNs in Section 6.

**Entropy** increases into the chaotic regime when  $r$  increases towards higher activity (i.e.  $r \rightarrow 0.5$ , see Fig. 4b and Fig. 6b). For fixed  $r$ : using destination randomization, increases in  $\gamma$  have little effect on the entropy, while with source randomization, increasing  $\gamma$  increases the entropy. It seems that while randomness in the topology does serve to increase the entropy, this is cannibalized in the destination randomized networks

---

(see  $r = 0.3, \bar{K} = 3$  with  $\gamma = 1.0$  in Fig. 2a and with  $\gamma = 0.0$  in Fig. 5 for the larger  $N = 264$  networks in this paper). In order to study transitions with respect to  $\gamma$  one may need to comprehensively evaluate such dependencies at different points, e.g. for larger  $K$  and/or less biased  $r$ , since as we have shown the full dynamical transition with respect to  $\gamma$  cannot be observed for every  $(r, \bar{K})$  combination.

by the known tendency of more broad in-degree distributions to show more ordered behavior [55]. As previously observed for  $\sigma_\delta$ , this does not seem to alter the boundary of the order-chaos transition though.

Crucially, **information storage** dominates the ordered phase of dynamics (with small activity  $r$  and low levels of rewiring  $\gamma$ ), shown in Fig. 4c, while **transfer** (captured in total in the entropy rate) dominates the chaotic phase (with large  $r$  and  $\gamma$ ), shown in Fig. 4d. The contrast between the two operations and phases is displayed well in Fig. 7. It is evident that the topological “crossover” between regular networks (such as lattices or “large worlds”) and random networks is approximately mirrored by the “crossover” between domination of information storage and then information transfer. These results imply that **information storage is strongly supported by the clustering or community structure in regular or locally-connected networks, while information transfer is strongly supported by the introduction of long links as the network is randomized**. This result is quite intuitive: high clustering could be expected to support the local storage and reinforcement of common information between neighbors (i.e. with distributed storage supported via self-communication through these clustered causal loops), while long links would be expected to provide new information to destination nodes that they would not receive from spatially-close sources. We note there is little difference in these trends if we turn our attention to source randomization (see Fig. 6c and Fig. 6d), save for the entropy rate increasing more strongly deeply in the chaotic regime, for the reasons described for the entropy above.

For the intervening values of  $r$  and  $\gamma$  **around the critical regime** in dynamics, the average information storage and transfer are **somewhat balanced**. Certainly there is some variation across sample networks; as shown in Fig. 8, it is possible for sample networks near the critical regime to have somewhat imbalanced storage and transfer. Importantly though, we see that balance between the two is only possible near the critical regime, and we expect the variation in the averages across sample networks to vanish in the limit of infinite network size. As such, since the critical regime occurs in similar regions to small-world networks, it could be said that **small-world networks have a propensity to balance information storage and transfer capabilities**.

**Information storage** peaks just inside the ordered phase of dynamics with respect to  $r$  for fixed  $\gamma$ , while for fixed  $r$  the storage decreases as  $\gamma$  is increased. This is shown for destination randomization in Fig. 4c, and also from another perspective in Fig. 9a; there is little difference for source randomization in Fig. 6c. Informa-

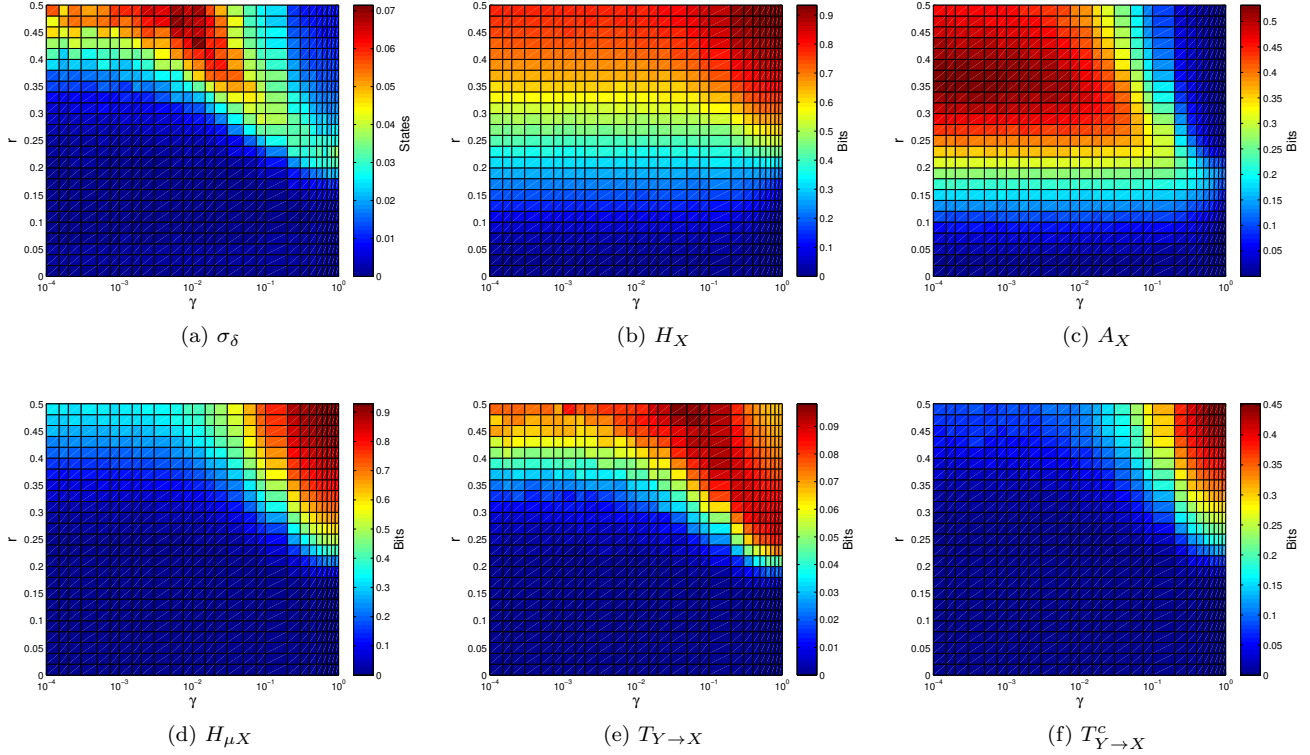


Figure 6: **Small-world and activity-driven transitions for randomized sources** (color online). Measures of dynamics versus  $r$  and  $\gamma$  for  $K = 4$  (i.e. ordered, small-world and random networks). We plot: (a) standard deviation of the convergence/divergence parameter  $\delta$ , the maxima of which indicates the location of the critical regime (the sign of  $\delta$ , not shown, indicates chaotic behavior in the top right for large  $\gamma$  and  $r$ , and ordered behavior for small  $\gamma$  and  $r$ ); (b) average entropy; (c) average active information storage; (d) average entropy rate; (e) apparent transfer entropy; and (f) complete transfer entropy. For an indication of the scale of error bars, see Fig. 7b.

tion storage shows no peak with respect to  $\gamma$  but only drops, since it is the large clustering in regular networks that strongly supports this operation. (In contrast, the drop at low  $r$  is due to lower activity caused by that parameter.)

The **apparent transfer entropy** peaks just inside the chaotic phase of dynamics, as shown for destination randomization in Fig. 4e, and also from another perspective in Fig. 9b. This result is also quite intuitive: as more long links are introduced, it becomes easier for information to be transferred across the network. However, with too many long links or randomization in structure, the large degree of interactions occurring means that it becomes more difficult to discern the *coherent* effect of a single source on a destination, and the apparent TE drops. Importantly, the result indicates that **single-source or coherent information transfer is maximized near the small-world regime**. This aligns with conjecture that long links in small-world networks increase the global efficiency of information transport [22], though we observe here that such efficiency with respect to coherent transfer becomes cannibalized with too many long links. For source randomization, we see in Fig. 6e and Fig. 9c that the peak is stronger with respect to  $r$  for fixed  $\gamma$ , and slightly weaker with respect to  $\gamma$  for fixed  $r$  (since the dynamics are less chaotic for high  $\gamma$  with the more broad in-degree).

As the dynamics move more deeply into the chaotic phase (with large  $r$  and  $\gamma$ ), **higher order interactions** begin to dominate, leading to a continued increase in overall transfer (captured by the entropy rate). Within this overall transfer component, the apparent TE decreases (Fig. 4e and Fig. 6e), and more of the transfer component is carried in higher order terms including the complete TE (Fig. 4f and Fig. 6f). This continued increase in overall transfer with network randomization could explain why random networks are most conducive to synchronization of coupled maps [4]. Note that the complete TE slightly decreases at large values of  $\gamma$  for destination randomization in Fig. 4f, while it was only observed to increase for source randomization in Fig. 6f and with respect to  $r$  in RBNs. This is caused by the broader distribution of in-degrees with larger  $\gamma$  for destination randomization in two ways: (i) as explained for the entropy, this distribution means the dynamics are somewhat less chaotic, and (ii) the transfer component is spread amongst more higher order terms. This effect does not occur for changes in  $r$ , meaning that the complete TE simply increases into the chaotic regime there.

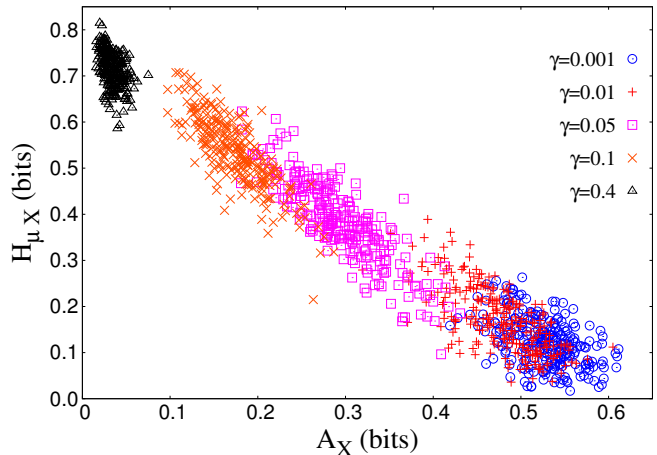


Figure 8: Average entropy rate  $H_{\mu X}$  versus active information storage  $A_X$  for each sample network studied for  $\bar{K} = 4$ ,  $r = 0.36$  and various values of  $\gamma$  ( $\gamma = 0.05$  is the closest to the critical regime of dynamics here). We have  $H_X = H_{\mu X} + A_X$  from Eq. (5), showing that these are the information transfer and storage components of the total information in a node  $X$  respectively. The trend in the plot approximates a straight line since  $H_X$  is almost constant with  $\gamma$  here (see Fig. 7).

### 6.3 Correlation of information dynamics to topological properties

In previous section we reported similarities between information-theoretic and topological measures in terms of their behavior around critical points. In order to investigate these relationships further, we compute correlations between (i) active information storage and clustering coefficient; and (ii) the entropy rate and the average path length.

Specifically, Fig. 10 shows the correlation of active information storage  $A_X(r, \bar{K}, \gamma)$  against clustering coefficient  $C(\bar{K}, \gamma)$  as  $\gamma$  is varied, plotted as a function of  $r$  and  $K$ . We see a very strong correlation of the clustering coefficient and the active information storage.<sup>13</sup> This provides further evidence that the local structure in the ordered networks is a large factor supporting the capacity for information storage there. As suggested earlier, this is reasonable, since highly clustered networks would provide structures by which nodes can more easily distribute storage amongst their neighbors.

Similarly, we see negative correlations between the entropy rate  $H_{\mu X}(r, \bar{K}, \gamma)$  (capturing the total amount of information that is contributed from neighboring

<sup>13</sup> This does not occur for  $\bar{K} = 2$  where the clustering coefficient does not capture the local-nature of the links.

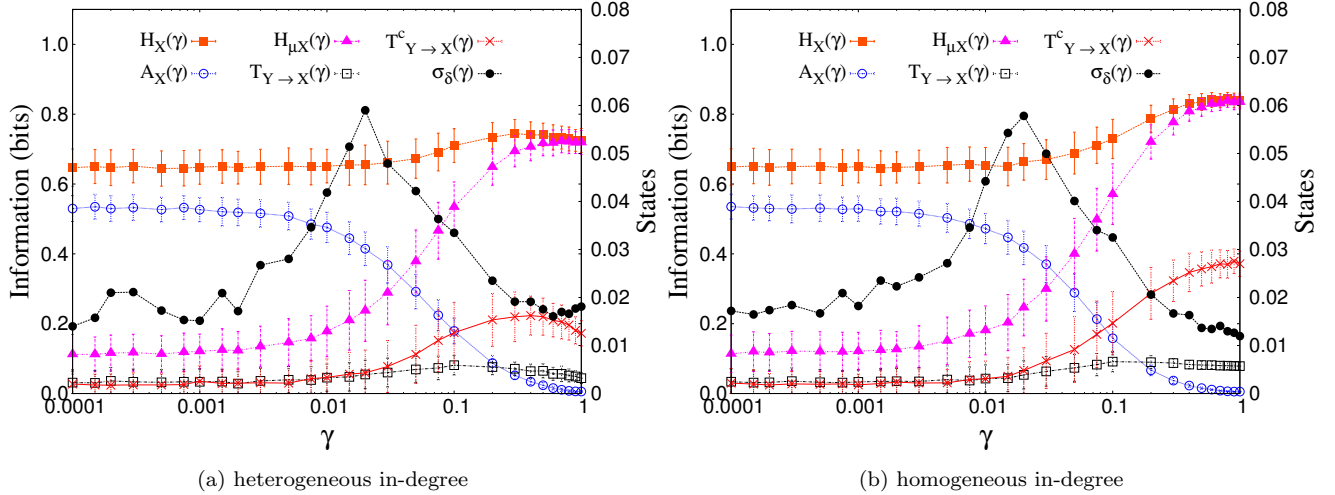


Figure 7: Information dynamics versus  $\gamma$ , for networks with  $\bar{K} = 4$  and  $r = 0.36$ , with (a) randomization of the destination of links (giving a heterogeneous in-degree distribution), and (b) randomization of the source of links (giving a homogeneous in-degree distribution). Information dynamics ( $H_X$ ,  $A_X$ ,  $H_{\mu X}$ ,  $T_{Y \rightarrow X}$  and  $T_{Y \rightarrow X}^C$ ) are in bits and plotted against the left y-axis. The standard deviation  $\sigma_\delta$  of the convergence/divergence parameter is plotted against the right y-axis. Through this small-world transition, we see a shift from ordered dynamics dominated by information storage to chaotic dynamics dominated by information transfer. Error bars indicate the *standard deviation* of the values across the 250 sampled networks. (The standard error of the mean is too small to be visible.)

sources here) and the average path length  $L(\bar{K}, \gamma)$  (not shown). This provides quantitative evidence for the suggestions that by bridging the distance between far-away neighbors, the network allows new information to be shared more easily across the network, providing a larger capacity for information transfer.

## 7 Conclusion

We have described results which quantify the fundamental nature of computation in small-world networks, as compared to regular and random topologies. For this investigation, we used Boolean dynamics, and as such the models we investigated were small-world Boolean networks, or random<sup>14</sup> Boolean networks spatially-embedded onto a small-world ring lattice.

In establishing a basis for our results, we found order-chaos phase transitions in dynamics, with respect to standard RBN parameters (connectivity and activity) and also with respect to the small-world topological transition driven by the rewiring parameter. The critical regime was approximately around the small-world transition region in topology, however this was strongly dependent on the level of activity in the dynamics. We then found that the ordered phase of these dynamics

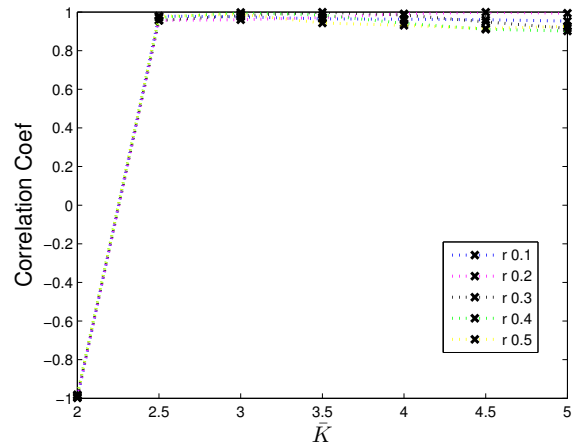
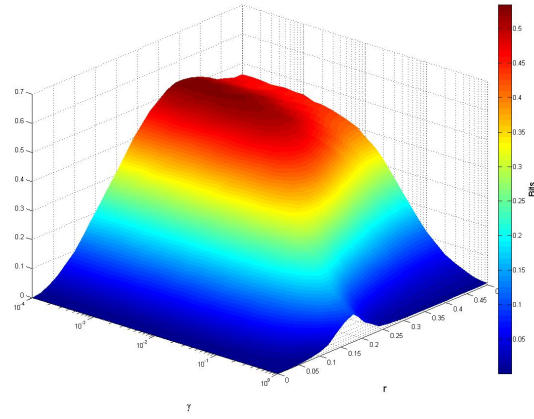
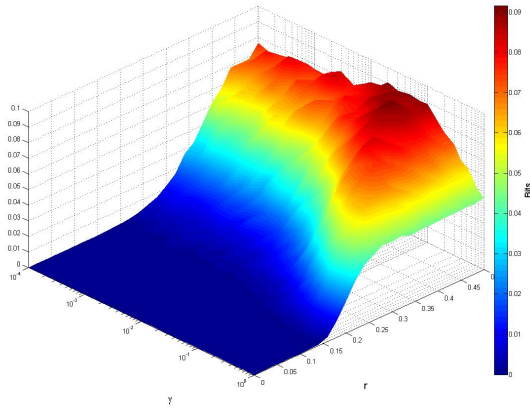


Figure 10: Correlation of active information storage  $A_X(r, \bar{K}, \gamma)$  against clustering coefficient  $C(\bar{K}, \gamma)$  (measured while  $\gamma$  is varied for destination randomization), plotted as a function of  $r$  and  $\bar{K}$ .

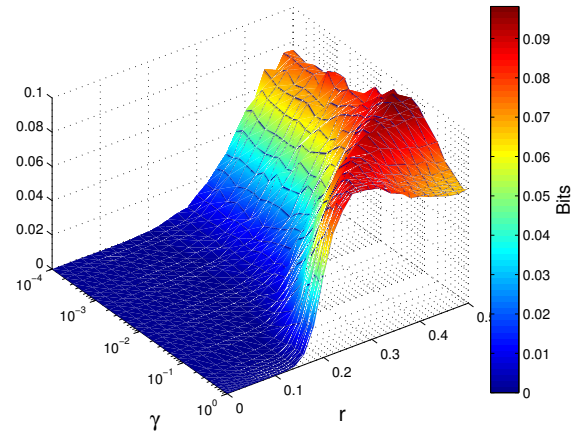
<sup>14</sup> Random in function, but not in topology now.



(a)  $A_X$



(b)  $T_{Y \rightarrow X}$



(c)  $T_{Y \rightarrow X}$

Figure 9: (color online) Measures of dynamics versus  $r$  and  $\gamma$  for  $K = 4$  (i.e. ordered, small-world and random networks): we plot (a) average active information storage and (b) apparent transfer entropy for destination randomization with probability  $\gamma$ , and (c) apparent transfer entropy for source randomization.

(low activity and low randomness in topology) is dominated by information storage, while the chaotic phase of the dynamics (high activity and high randomness in topology) is dominated by information transfer. The critical regime in dynamics exhibited a balance between these two operations. Since the critical regime was near to the small-world regime in topology, it could be said that small-world networks have a propensity to combine comparably large information storage and transfer capabilities.

Furthermore, this balance for small-world networks can be explained by considering how the topological features related to the information dynamics on the network. We found information storage to be strongly correlated to the clustering coefficient: locally clustered structure appears to provide strong support for information storage operations. In contrast, information transfer was anti-correlated with path length: long links appear to be a crucial facilitator of information transfer across the network. Additionally, we found that single-source or coherent information transfer is maximized slightly inside the chaotic phase of dynamics (near to the small-world regime), with the capacity for coherent computation being eroded as too many random links raise the level of interactions and push the dynamics further into the chaotic regime. Finally, we found subtle differences depending on whether we randomized the sources or destinations of edges, though the general conclusions hold for both approaches.

These findings are quite significant, as they provide the first direct quantitative investigation of these intrinsic properties of distributed computation on small-world networks. If one considers that complex computation requires both strong information storage and transfer capability, then the results could be seen to add evidence for findings that small-world networks hold computational advantages over other topologies [18, 22, 46, 47, 48, 51].

In future work, we will investigate the computational properties of other network topologies, and in particular examine these on a local scale. Furthermore, we are investigating the behavior of other complexity measures applied to RBNs, for example the Fisher information [12], which measures how much a system's dynamics reveals about its parameters [49, 50].

## 8 Acknowledgements

We would like to thank the CSIRO High Performance Computing and Communications Centre (<http://www.hpccc.gov.au/>) and the Max Planck Institute for Mathematics in the Sciences for the use of their supercomputer clusters in performing the experi-

ments for this paper.

The measures of network topology (path length and clustering coefficient) were computed using the Brain connectivity toolbox [43].

The authors thank Qianchuan Zhao for clarifying the results from [55].

## References

- [1] Aldana, M. (2003) Boolean dynamics of networks with scale-free topology. *Physica D*, **185**, 45–66.
- [2] Amaral, L. A. N., Scala, A., Barthélemy, M., and Stanley, H. E. (2000) Classes of small-world networks. *Proceedings of the National Academy of Sciences of the United States of America*, **97**, 11149–11152.
- [3] Argollo de Menezes, M., Moukarzel, C. F., and Penna, T. J. P. (2000) First-order transition in small-world networks. *Europhysics Letters*, **50**, 574.
- [4] Atay, F. M., Jost, J., and Wende, A. (2004) Delays, connection topology, and synchronization of coupled chaotic maps. *Physical Review Letters*, **92**, 144101.
- [5] Barabási, A.-L. (2009) Scale-free networks: A decade and beyond. *Science*, **325**, 412–413.
- [6] Barthélemy, M. and Amaral, L. A. N. (1999) Small-world networks: Evidence for a crossover picture. *Physical Review Letters*, **82**, 3180–3183.
- [7] Damiani, C., Kauffman, S., Serra, R., Villani, M., and Colacci, A. (2010) Information transfer among coupled random Boolean networks. Bandini, S., Manzoni, S., Umeo, H., and Vizzari, G. (eds.), *Cellular Automata*, vol. 6350 of *Lecture Notes in Computer Science*, pp. 1–11, Springer Berlin / Heidelberg.
- [8] Darabos, C., Giacobini, M., and Tomassini, M. (2007) Semi-synchronous activation in scale-free Boolean networks. Almeida e Costa, F., Rocha, L. M., Costa, E., Harvey, I., and Coutinho, A. (eds.), *Proceedings of the 9th European Conference on Artificial Life (ECAL 2007)*, Lisbon, Portugal, Berlin / Heidelberg, vol. 4648 of *Lecture Notes in Artificial Intelligence*, pp. 976–985, Springer.
- [9] Derrida, B. and Pomeau, Y. (1986) Random networks of automata: a simple annealed approximation. *Europhysics Letters*, **1**, 45–49.
- [10] Erdős, P. and Rényi, A. (1961) On the evolution of random graphs. *Bull. Inst. Internat. Statist.*, **38**, 343–347.
- [11] Feldman, D. P. and Crutchfield, J. P. (2003) Structural information in two-dimensional patterns: Entropy convergence and excess entropy. *Physical Review E*, **67**, 051104.
- [12] Fisher, R. A. (1922) On the mathematical foundations of theoretical statistics. *Philosophical Transactions of the Royal Society, A*, **220**, 309–368.
- [13] Flyvbjerg, H. (1988) An order parameter for networks of automata. *Journal of Physics A: Mathematical and General*, **21**, L955.
- [14] Gershenson, C. (2003), RBNLab. Online software: <http://rbn.sourceforge.net>.

- [15] Gershenson, C. (2004) Introduction to random Boolean networks. Bedau, M., Husbands, P., Hutton, T., Kumar, S., and Suzuki, H. (eds.), *Proceedings of the Workshops and Tutorials of the Ninth International Conference on the Simulation and Synthesis of Living Systems (ALife IX)*, Boston, USA, pp. 160–173.
- [16] Gershenson, C. (2004), Phase transitions in random Boolean networks with different updating schemes. ArXiv:nlin/0311008.
- [17] Gershenson, C. (2004) Updating schemes in random Boolean networks: Do they really matter? Pollack, J., Bedau, M., Husbands, P., Ikegami, T., and Watson, R. A. (eds.), *Proceedings of the Ninth International Conference on the Simulation and Synthesis of Living Systems (ALife IX)*, Boston, USA, Cambridge, USA, pp. 238–243, MIT Press.
- [18] Katare, S. and West, D. H. (2006) Optimal complex networks spontaneously emerge when information transfer is maximized at least expense: A design perspective. *Nature Physics*, **11**, 26–35.
- [19] Kauffman, S. A. (1993) *The Origins of Order: Self-Organization and Selection in Evolution*. Oxford University Press.
- [20] Kinouchi, O. and Copelli, M. (2006) Optimal dynamical range of excitable networks at criticality. *Nature Physics*, **2**, 348–351.
- [21] Langton, C. G. (1990) Computation at the edge of chaos: phase transitions and emergent computation. *Physica D*, **42**, 12–37.
- [22] Latora, V. and Marchiori, M. (2001) Efficient behavior of small-world networks. *Physical Review Letters*, **87**, 198701.
- [23] Lizier, J. T., Prokopenko, M., and Cornforth, D. J. (2009) The information dynamics of cascading failures in energy networks. *Proceedings of the European Conference on Complex Systems (ECCS)*, Warwick, UK, p. 54, ISBN: 978-0-9554123-1-8.
- [24] Lizier, J. T. and Prokopenko, M. (2010) Differentiating information transfer and causal effect. *European Physical Journal B*, **73**, 605–615.
- [25] Lizier, J. T., Prokopenko, M., and Zomaya, A. Y. (2007) Detecting non-trivial computation in complex dynamics. Almeida e Costa, F., Rocha, L. M., Costa, E., Harvey, I., and Coutinho, A. (eds.), *Proceedings of the 9th European Conference on Artificial Life (ECAL 2007)*, Lisbon, Portugal, Berlin / Heidelberg, vol. 4648 of *Lecture Notes in Artificial Intelligence*, pp. 895–904, Springer.
- [26] Lizier, J. T., Prokopenko, M., and Zomaya, A. Y. (2008) The information dynamics of phase transitions in random Boolean networks. Bullock, S., Noble, J., Watson, R., and Bedau, M. A. (eds.), *Proceedings of the Eleventh International Conference on the Simulation and Synthesis of Living Systems (ALife XI)*, Winchester, UK, Cambridge, MA, pp. 374–381, MIT Press.
- [27] Lizier, J. T., Prokopenko, M., and Zomaya, A. Y. (2008) Local information transfer as a spatiotemporal filter for complex systems. *Physical Review E*, **77**, 026110.
- [28] Lizier, J. T., Prokopenko, M., and Zomaya, A. Y. (2010) Information modification and particle collisions in distributed computation. *Chaos*, **20**, 037109.
- [29] Lizier, J. T., Prokopenko, M., and Zomaya, A. Y. (2011) Local measures of information storage in complex distributed computation, under submission.
- [30] Lizier, J. T. (2010) *The local information dynamics of distributed computation in complex systems*. Ph.D. thesis, The University of Sydney.
- [31] Lu, Q. and Teuscher, C. (2009), Damage spreading in spatial and small-world random Boolean networks. arXiv:0904.4052.
- [32] Luque, B., Blanc, C., and Solé, R. V. (1997) Order parameters, Lyapunov exponents, and control in random Boolean networks. Working Paper 97-11-084, Santa Fe Institute.
- [33] MacKay, D. J. (2003) *Information Theory, Inference, and Learning Algorithms*. Cambridge University Press.
- [34] Mitchell, M. (2006) Complex systems: Network thinking. *Artificial Intelligence*, **170**, 1194–1212.
- [35] Newman, M. and Watts, D. J. (1999) Renormalization group analysis of the small-world network model. *Physics Letters A*, **263**, 341–346.
- [36] Oosawa, C. and Savageau, M. A. (2002) Effects of alternative connectivity on behavior of randomly constructed Boolean networks. *Physica D*, **170**, 143–161.
- [37] Rämö, P., Kauffman, S., Kesseli, J., and Yli-Harja, O. (2007) Measures for information propagation in Boolean networks. *Physica D*, **227**, 100–104.
- [38] Ribeiro, A. S., Kauffman, S. A., Lloyd-Price, J., Samuelsen, B., and Socolar, J. E. S. (2008) Mutual information in random Boolean models of regulatory networks. *Physical Review E*, **77**, 011901–10.
- [39] Rohlf, T. and Bornholdt, S. (2009) Self-organized criticality and adaptation in discrete dynamical networks. Gross, T. and Sayama, H. (eds.), *Adaptive Networks - Theory, Models and Applications*, Berlin / Heidelberg, vol. 4850, pp. 73–108, Springer.
- [40] Rohlf, T., Gulbahce, N., and Teuscher, C. (2007) Damage spreading and criticality in finite random dynamical networks. *Physical Review Letters*, **99**, 248701.
- [41] Schreiber, T. (2000) Measuring information transfer. *Physical Review Letters*, **85**, 461–464.
- [42] Solé, R. V. and Valverde, S. (2001) Information transfer and phase transitions in a model of internet traffic. *Physica A*, **289**, 595–605.
- [43] Sporns, O., Rubinov, M., and Kötter, R. (2009), Brain connectivity toolbox. Online software: <http://www.brain-connectivity-toolbox.net/>.
- [44] Stauffer, D. (1989) Hunting for the fractal dimension of the Kauffman model. *Physica D: Nonlinear Phenomena*, **38**, 341–344.
- [45] Stauffer, D. (1994) Evolution by damage spreading in Kauffman model. *Journal of Statistical Physics*, **74**, 1293–1299.
- [46] Tassier, T. and Menczer, F. (2001) Emerging small-world referral networks in evolutionary labor markets. *IEEE Transactions on Evolutionary Computation*, **5**, 482–492.

- [47] Teuscher, C. (2006) On irregular interconnect fabrics for self-assembled nanoscale electronics. *Proceedings of the 2<sup>nd</sup> IEEE International Workshop on Default and Fault Tolerant Nanoscale Architectures, NANOARCH'06*, Boston, MA, USA, pp. 60–67.
- [48] Tomassini, M., Giacobini, M., and Darabos, C. (2005) Evolution and dynamics of small-world cellular automata. *Complex Systems*, **15**, 261–284.
- [49] Wang, X. R., Lizier, J. T., and Prokopenko, M. (2010) A Fisher information study of phase transitions in random Boolean networks. Fellermann, H., Dörr, M., Hanczyc, M. M., Laursen, L. L., Maurer, S., Merkle, D., Monnard, P.-A., Stoy, K., and Rasmussen, S. (eds.), *Proceedings of the 12th International Conference on the Synthesis and Simulation of Living Systems (Alife XII)*, Odense, Denmark, Cambridge, MA, pp. 305–312, MIT Press.
- [50] Wang, X. R., Lizier, J. T., and Prokopenko, M. (2011) Fisher information at the edge of chaos in random Boolean networks. *Artificial Life*, in press.
- [51] Watts, D. J. and Strogatz, S. (1998) Collective dynamics of ‘small-world’ networks. *Nature*, **393**, 440–442.
- [52] Wuensche, A. (1997) *Attractor Basins of Discrete Networks*. Ph.D. thesis, The University of Sussex.
- [53] Wuensche, A. (1999) Classifying cellular automata automatically: Finding gliders, filtering, and relating space-time patterns, attractor basins, and the Z parameter. *Complexity*, **4**, 47–66.
- [54] Yuan, W.-J., Luo, X.-S., Jiang, P.-Q., Wang, B.-H., and Fang, J.-Q. (2008) Transition to chaos in small-world dynamical network. *Chaos, Solitons & Fractals*, **37**, 799–806.
- [55] Zhang, X. and Zhao, Q. (2009) Effects of small world topology on the critical boundary for Boolean networks. *Physica A*, **388**, 3657–3666.